2900-239-T

Report of Project MICHIGAN

X-BAND LADDER-LINE TRAVELING-WAVE MASER

G. I. HADDAD
J. E. ROWE

February 1961

Institute of Science and Technology
THE UNIVERSITY OF MICHIGAN
Ann Arbor, Michigan

NOTICES

Sponsorship. The work reported herein was conducted by the Institute of Science and Technology for the U. S. Army Signal Corps under Project MICHIGAN, Contract DA-36-039 SC-78801. Contracts and grants to The University of Michigan for the support of sponsored research by the Institute of Science and Technology are administered through the Office of the Vice-President for Research.

Distribution. Initial distribution is indicated at the end of this document. Distribution control of Project MICHIGAN documents has been delegated by the U. S. Army Signal Corps to the office named below. Please address correspondence concerning distribution of reports to:

U. S. Army Liaison Group
Project MICHIGAN
The University of Michigan
P. O. Box 618
Ann Arbor, Michigan

ASTIA Availability. Qualified requesters may obtain copies of this document from:

Armed Services Technical Information Agency
Arlington Hall Station
Arlington 12, Virginia

Final Disposition. After this document has served its purpose, it may be destroyed. Please do not return it to the Institute of Science and Technology.

PREFACE

Project MICHIGAN is a continuing research and development program for advancing the Army's long-range combat-surveillance and target-acquisition capabilities. The program is carried out by a full-time Institute of Science and Technology staff of specialists in the fields of physics, engineering, mathematics, and psychology, by members of the teaching faculty, by graduate students, and by other research groups and laboratories of The University of Michigan.

The emphasis of the Project is upon basic and applied research in radar, infrared, information processing and display, navigation and guidance for aerial platforms, and systems concepts. Particular attention is given to all-weather, long-range, high-resolution sensory and location techniques, and to evaluations of systems and equipments both through simulation and by means of laboratory and field tests.

Project MICHIGAN was established at The University of Michigan in 1953. It is sponsored by the U. S. Army Combat Surveillance Agency of the U. S. Army Signal Corps. The Project constitutes a major portion of the diversified program of research conducted by the Institute of Science and Technology in order to make available to government and industry the resources of The University of Michigan and to broaden the educational opportunities for students in the scientific and engineering disciplines.

Progress and results described in reports are continually reassessed by Project MICHIGAN. Comments and suggestions from readers are invited.

Robert L. Hess
Technical Director
Project MICHIGAN

CONTENTS

FIGURES

X-BAND LADDER-LINE TRAVELING-WAVE MASER

ABSTRACT

The factors to be considered in the design of a broadband traveling-wave solid-state maser are outlined, with particular consideration given to the choice of an rf propagating structure. Desirable structure characteristics for a TWM (traveling-wave maser) are low loss, high slowing, ease of coupling between the pump signal and the paramagnetic crystal, simple, rugged construction, and easily accessible regions of different senses of circular polarization of the rf magnetic field.

An X-band ruby TWM has been constructed and tested in which the rf structure is a double-ridge ladder line and the signal is coupled into and out of the structure with coaxial lines. The pump power is propagated in a waveguide mode and the device is operated at and below liquid-helium temperatures. A 4-inch electromagnet was used. The TWM was operated at the push-pull point with a pump frequency of 24 kmc and a signal frequency of approximately 9.65 kmc; the magnetic field was 4.1 kilogauss.

Gross gains of 15 db have been obtained and bandwidths as high as 130 mc were observed. Reduced structure losses and longer sections of ruby promise a square-root voltage gain times the bandwidth ($G^{1/2}B$) of 1100 mcs (30 db over 35 mc).

1 INTRODUCTION

In 1956, Bloembergen proposed an excitation scheme through which continuous microwave amplification could be obtained by utilizing three energy levels of a paramagnetic material, called the three-level solid-state maser (Reference 1). This scheme employs a microwave pump signal to transform the material from an absorptive to an emissive state when such a material is stimulated by radiation at the signal frequency. His prediction that it would exhibit very low noise characteristics generated a great deal of interest in the maser, and since then this principle has been successfully utilized to construct maser amplifiers of both the cavity and traveling-wave types (References 2 through 6).

In a cavity maser the microwave radiation is coupled to the paramagnetic salt by making the cavity, containing the paramagnetic salt, resonant at both the signal and pump frequencies. Such masers, however, do not utilize the full line width of the material because of the high degree of regeneration required to obtain a significant amount of gain. This regeneration, in turn, limits the bandwidth of operation. A measure of the performance of these systems is the product of the square-root voltage gain times the bandwidth in megacycles. Representative

values of $G^{1/2}B$ for cavity masers vary from 40 to 100 mcs. Various schemes such as resonant coupling and stagger tuning several cavities have been proposed to increase achievable values of $G^{1/2}B$. Square-root gain bandwidth products of 200-300 mcs have been obtained using resonant coupling of maser cavities at X-band.

A TWM, on the other hand, employs a slow-wave structure in place of the resonant cavities and should permit larger instantaneous bandwidths. The velocity of energy propagation along the rf structure can be made very low so that effective coupling between the microwave radiation and the spins of the paramagnetic salt can be obtained. Unidirectional gain can be obtained if a slow-wave structure which has separated accessible regions of circular polarization of the rf magnetic field is chosen. A material with circularly polarized signal frequency transitions can then be located in the structure in such a manner that coupling between the rf field and the material is obtained for only one direction of propagation. When the material is located in this way, and a pump signal of the proper frequency is employed, the material exhibits a negative resistance as viewed from the rf structure and an exponential growing wave results in the one direction, while little or no growth is obtained in the reverse direction.

Unidirectional loss can also be incorporated in the structure in the same manner as gain. A high degree of isolation can be obtained by using either a highly doped paramagnetic material, whose thermal equilibrium cannot be disturbed by the pump power, or a ferrimagnetic material such as yttrium iron garnet.

Because unidirectional gain and loss can be obtained in a TWM, freedom from regenerative instability can be insured with the result that the TWM has a higher degree of gain stability than the cavity maser. This is of great practical importance in many systems applications; e.g., in radiometers and radio telescopes.

Since the passband of the slow-wave structure can be made much larger than the material line width as defined by the magnetic susceptibility curve, full utilization of the line width can be achieved so that a larger instantaneous bandwidth than that of the cavity results. Another advantage of the TWM is the possibility of electronic tuning over a wider frequency range. This tuning is accomplished by changing the pump frequency and the d-c magnetic field.

2
TRAVELING-WAVE MASER THEORY

The gain expression for a TWM has been derived in the literature (Reference 5). One form is:

$$G_{db} = \frac{27.3SN}{Q_m} \tag{1}$$

where $S = \frac{c}{v_g}$ = the electromagnetic wave slowing factor

$N = \frac{\ell}{\lambda_0}$ = the number of free-space wavelengths along the structure

Q_m = the magnetic Q, determined by the material and the filling factor in the structure

c and v_g = the velocities of light and of energy propagation along the structure, respectively

It is clear from Equation 1 that in order to obtain high gain, the slowing factor should be as high as possible and the magnetic Q as low as possible for the frequencies of interest. For a typical magnetic Q of 150, a slowing factor of 50, and a structure length of 4 inches, a gain of approximately 30 db at 10 kmc can be obtained.

It has also been shown by Degrasse et al. (Reference 5) that, assuming a Lorentzian line shape, the 3-db bandwidth of a TWM is approximately given by

$$B = B_m \sqrt{\frac{3}{G_{db} - 3}} \tag{2}$$

where B_m is the frequency bandwidth over which the imaginary part of the complex permeability is greater than one-half its peak value. For a gain of 30 db the bandwidth is approximately equal to 0.335 B_m. B_m depends on both the material and the point of maser operation that is employed. For ruby, which has been found to be a good maser material, a typical value of B_m at 6 kmc and at an angle of 90^o between the d-c magnetic field and the ruby c-axis is approximately 60 mc. At the push-pull point and for X-band maser operation, B_m is of the order of 120 mc. Thus a gain of 30 db over a bandwidth of more than 35 mc would be obtained at this point of operation.

The group velocity in a slow-wave structure can be related to the pitch and the width of the passband as follows. For the fundamental mode of a periodic structure operating in the passband, the phase shift per section varies between $\beta L = 0$ and $\beta L = \pi$, where L is the pitch and βL is the phase shift per section. Therefore,

$$v_g = \frac{d\omega}{d\beta} = \frac{\Delta\omega}{\Delta\beta} = \frac{2\pi\Delta f}{\Delta\beta} = 2L\Delta f \tag{3}$$

The slowing factor S of Equation 1 can then be written as

$$S = \frac{c}{v_g} = \frac{c}{2L\Delta f} = \left(\frac{\lambda_0}{2L}\right)\left(\frac{f_0}{\Delta f}\right) \tag{4}$$

It can easily be seen from Equation 4 that the smaller the pitch and the passband the higher the slowing factor. Since the gain in the TWM is directly proportional to the slowing factor, both the pitch and the passband of the slow-wave structure must be made as small as possible. This requirement results in TWM rf structures which have a very small pitch for a given frequency.

3
MASER SLOW-WAVE STRUCTURES

A slow-wave structure which is suitable for TWM operation must possess the following characteristics:

(1) The structure must be designed so that a high degree of slowing is achieved in the signal energy propagation along the structure; i.e., high slowing factors should be obtainable in such a structure.

(2) It must possess different senses of circular polarization of the rf magnetic field in different regions which are readily accessible. This makes unilateral gain and loss possible.

(3) The insertion loss due to ohmic losses in the structure must be as small as possible. This, of course, will improve the net gain of the amplifier.

(4) The structure must be constructed so that provision can be made to allow effective coupling between the pump signal and the paramagnetic material. This could be in the form of either a broadband resonant mode or a propagating mode.

(5) Relatively large size (compared with λ_0), ease of manufacturing, ruggedness, and easy means of coupling the signal power into and out of the structure conclude the list of features a slow-wave structure must have to be applicable in a TWM scheme.

Several structures which have been discussed in the literature (Reference 5) possess the characteristics cited above and a few of them (References 4-6) have been successfully applied to construct TWM amplifiers. These amplifiers have been operated in the frequency range of 6 kmc and lower (References 4-6).

A double-ridge Karp structure has been employed at the Electron Physics Laboratory to develop a TWM at X-band frequencies. A detailed discussion of the characteristics of this structure and its utilization in a TWM is presented in the following sections.

There are several means for achieving significant wave slowing, including dielectric, geometric, resonant, and dispersive slowing. In dielectric slowing, perhaps the most familiar of these methods, the group velocity of the wave is proportional to $1/\sqrt{\epsilon_r}$. A slowing factor of 50 would therefore require a material with a dielectric constant of 2500. Since available materials with such a high dielectric constant are generally lossy, unstable, and temperature-sensitive, this method of slowing is not considered very practical. Materials such as titanium dioxide with an $\epsilon_r = 100$ are particularly useful in TWM's operating above X-band, where many free-space wavelengths can be obtained in a short physical distance. It is also desirable that the Q_m be relatively small. If dielectric slowing is used in a rectangular waveguide and if the energy is propagated in the TE_{10} mode, the size of the waveguide is also reduced by the square root of ϵ_r, which can become very tiny at high frequencies and thus very difficult to fabricate.

Geometric slowing is best exemplified by the helix, which is a nonresonant periodic rf structure. The wave travels in the direction of the helix wire with the velocity of light, while the axial phase velocity is reduced in proportion to the number of turns per wavelength. High slowing can be obtained in a helix over a large bandwidth. However, since the field configuration is not favorable, a spiraling d-c magnetic field would be required to orient the d-c field perpendicular to the circularly polarized rf field.

The various types of ladder structures, e.g., the interdigital line, the comb structure, and the Karp structure, are examples of resonant slowing. In these structures ladder elements extend from the walls into the region between the walls and in some cases are connected to the walls at both ends. Each period of the ladder structure is a resonant element, and the energy is reflected back and forth between the side walls in the form of a propagating TEM wave. These types of periodic structures have a definite passband with associated upper and lower cutoff frequencies. As shown in Equation 4, the narrower the passband in such structures and the smaller the pitch, the higher the slowing. As a result, slowing factors of very high magnitudes can be achieved in these structures. Limits do exist, however, because the passband of the structure must be at least as large as the material line width, and because the pitch must not be so small as to prevent effective interaction between the rf fields and a large number of spins. This lower pitch limit is due to the fact that, as the spacing between fingers becomes smaller, the fields become more tightly bound to the fingers.

Dispersive slowing is obtained by operating very close to the cutoff frequencies of a microwave filter, whether of the low-pass, high-pass, or bandpass type. Very high slowing factors can be obtained in such a region of operation, but the Q of the structure must be high to avoid excessive amounts of insertion loss.

4
KARP-TYPE SLOW-WAVE STRUCTURE

The Karp-type slow-wave structure consists of a planar array of conductors which are situated in a waveguide in such a manner that they are electrically connected to the side walls. The waveguide can be either double- (Figure 1b) or single-ridge (Figure 1c). When the ridges are not present the structure becomes nonpropagating, because the electric and magnetic couplings between adjacent rods cancel. Since this structure, known as the Easitron structure (Figure 1a), has a zero passband, it must be loaded in some manner to obtain a finite passband. The double-ridge Karp structure has been employed here in developing a TWM at X-band frequencies. The characteristics of the double-ridge structure are very similar to those of the single-ridge structure and will be discussed in detail in Section 6.

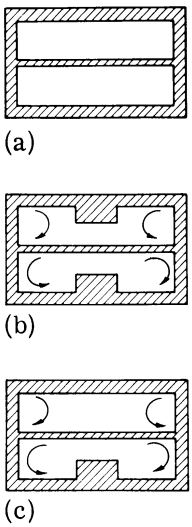

FIGURE 1. LADDER-LINE RF STRUCTURES. (a) Easitron nonpropagating structure. (b) Double-ridge Karp propagating structure. (c) Single-ridge Karp propagating structure. The arrows indicate the sense of circular polarization.

The Karp-type structure possesses all of the characteristics essential to a TWM application. Very high slowing factors can be obtained by adjusting the dimensions and by properly loading the structure with a dielectric which in this case can be the active maser material itself. The magnetic field has different senses of circular polarization above and below the plane of the fingers. Therefore, unilateral gain and attenuation can be obtained by placing the active

maser material and the isolation material below and above the fingers, respectively. The magnetic field intensity is maximum at the shorted ends of the fingers and zero in the middle. The electric field is maximum in the middle of the fingers and zero at the shorted ends. Thus, by placing a dielectric material such as ruby next to the side walls, effective magnetic coupling can be achieved without producing high dielectric loading, which might otherwise affect the structure characteristics considerably.

The microwave pump power, which is necessary to invert the spin population in the paramagnetic crystal, can be propagated in the ridged waveguide which encloses the ladder line. If this power propagates through the waveguide in a TE_{10} mode, and if the ladder line is placed in the middle of the waveguide (Figure 1b), a minimum amount of coupling between the waveguide mode and the ladder will result. The waveguide can be shorted at one end and a coupling iris placed at the other to enhance the coupling of the pumping field to the maser crystal.

The group velocity, which is needed to compute the gain, and the tunable bandwidth of the maser can be computed from the frequency vs. phase-shift-per-section characteristics of the slow-wave structure. Since these characteristics are essentially the same in the double- and single-ridge Karp structures, the phase vs. frequency characteristics of the single-ridge structure have been analyzed in detail. The effect of dielectric materials placed in different regions of the structure, namely, in the middle and at the sides, has also been considered.

Figure 2 shows a single-ridge Karp structure. The material on the sides has a relative dielectric constant, ϵ_{r_1}, which in this case is that of the active maser material, ruby, whose $\epsilon_r = 9$. The material between the ridge and the ladder has a relative dielectric constant ϵ_{r_2}. This material can be either rutile ($\epsilon_r \approx 100$) or air ($\epsilon_r = 1$).

A useful equivalent circuit for this structure is shown in Figure 3. The fingers are considered as two shorted transmission lines with a characteristic impedance of Z_0. L and C include the effects of the ridge and the dielectric material.

For the equivalent circuit of Figure 3, the lower frequency cutoff occurs when the admittance of the shunt arm is equal to zero. This can be expressed as

$$Y_{shunt} = \frac{1}{j2\pi f_c L} + j2\pi f_c C = 0 \tag{5}$$

where f_c is the lower cutoff frequency. L is then expressed as

$$L = \frac{1}{\omega_c^2 C} \tag{6}$$

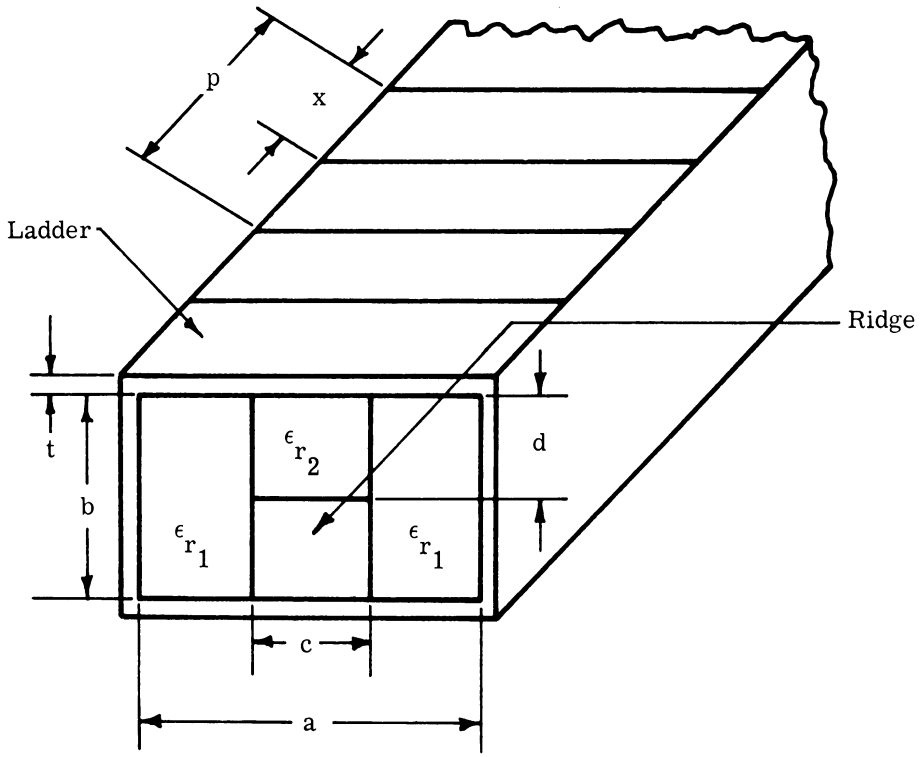

FIGURE 2. TWM STRUCTURE

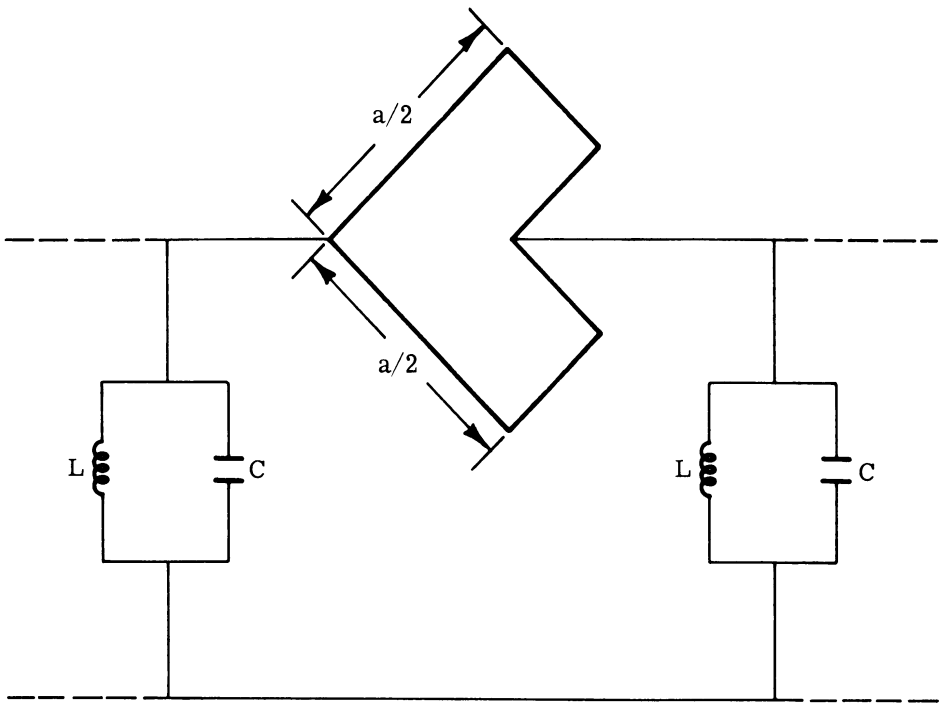

FIGURE 3. KARP STRUCTURE EQUIVALENT CIRCUIT

where $\omega_c = 2\pi f_c$. The susceptance of the shunt arm is conveniently written as

$$B_{shunt} = j\omega C\left[1 - \left(\frac{\omega_c}{\omega}\right)^2\right] \tag{7}$$

If the series arm in Figure 3 is considered as two shorted transmission lines in parallel, the susceptance of this arm, B_{series}, becomes

$$B_{series} = -j2Y_0 \cot\frac{\beta a}{2} \tag{8}$$

where a = the finger length

Y_0 = the characteristic admittance of the fingers considered as a transmission line

β = phase shift in radians per unit length

If f_1 is taken as the frequency at which the slot length a is one half a free-space wavelength, then Equation 8 becomes

$$B_{series} = -j2Y_0 \cot\left(\frac{\pi}{2}\frac{f}{f_1}\right) \tag{9}$$

Filter theory is used to relate the phase shift per section, θ, to the admittances of the series and the shunt arms through the expression

$$\cos\theta = 1 + \frac{B_{shunt}}{2B_{series}} \tag{10}$$

Substituting the values of B_{shunt} and B_{series} from Equations 7 and 9 into 10 yields

$$\cos\theta = 1 - 2\pi f\left(\frac{CZ_0}{4}\right)\left[1 - \left(\frac{f_c}{f}\right)^2\right]\tan\left(\frac{\pi}{2}\frac{f}{f_1}\right) \tag{11}$$

Thus for a certain f_c, f_1, and CZ_0, a phase shift vs. frequency curve can be obtained.

The lower cutoff frequency is determined by the waveguide dimensions, by the kind of dielectric material that is employed, and by the location of this material in the waveguide. The cutoff conditions in a ridged waveguide have been presented in the literature (References 7 and 8) and are plotted in Figure 4 for convenience. The cutoff conditions for a dielectric loaded waveguide, which are of interest here, have also been plotted in Figure 5. These graphs enable one to obtain the lower cutoff frequency of the structure and also the cutoff frequency of the TE_{20} mode, which is of interest when the pump power is propagated through the structure in a waveguide mode.

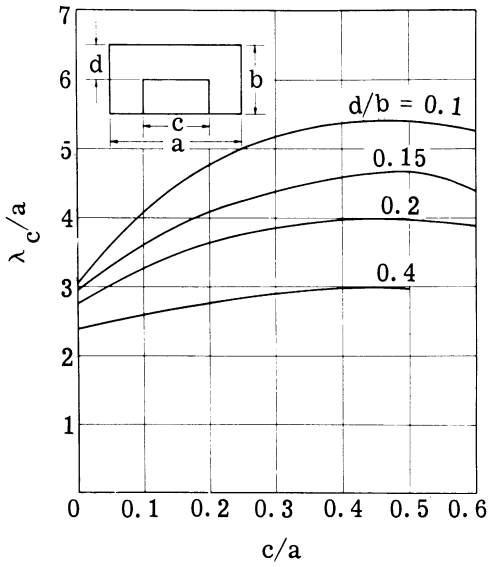

FIGURE 4. CUTOFF CONDITIONS OF THE TE_{10} MODE IN A RIDGED WAVEGUIDE b/a = 0.25.

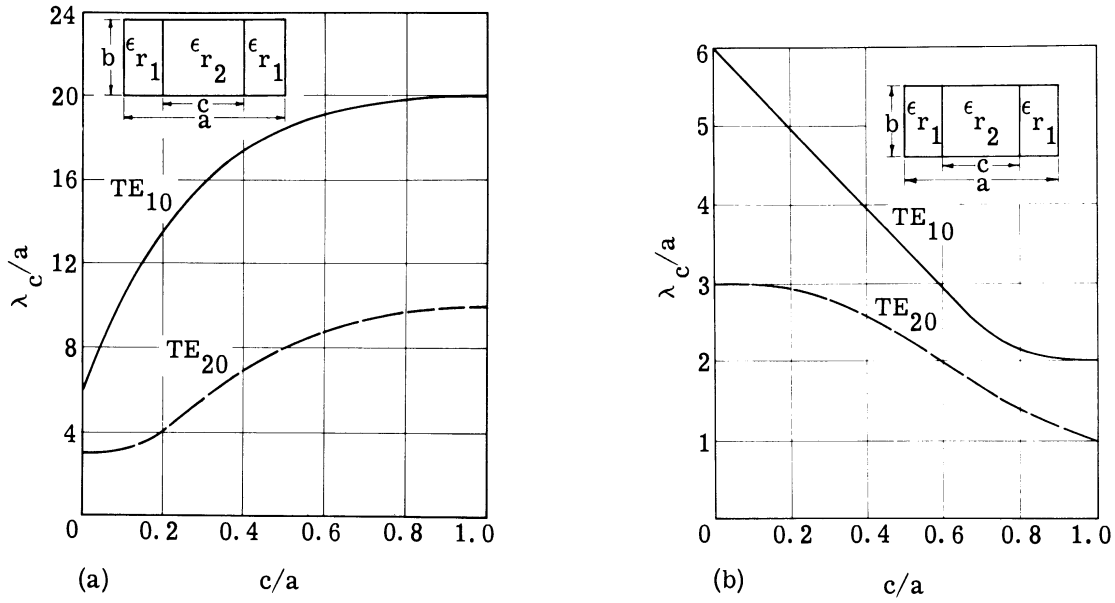

FIGURE 5. CUTOFF CONDITIONS FOR A DIELECTRIC LOADED WAVEGUIDE. (a) $\epsilon_{r_1} = 9$, $\epsilon_{r_2} = 100$. (b) $\epsilon_{r_1} = 9$, $\epsilon_{r_2} = 1$.

The frequency f_1 is fixed by a choice of the length of the fingers. This choice and the amount of capacitive loading that is introduced by the ridge and the dielectric determine the upper cutoff frequency of the slow-wave structure.

The amount of capacitive loading is measured by C, the capacitance of the shunt arm, and can be approximately expressed in terms of the dimensions and the dielectric constant through the expression

$$C \approx \frac{\epsilon c(p - x)}{d} \tag{12}$$

where p = the pitch of the ladder line

d = the distance between the ridge and the ladder

c = the width of the ridge

x = the width of the slot in the ladder

ϵ = the dielectric constant of the material between the ridge and the ladder

The above equation gives an approximate expression for C. The major contribution to C arises from loading at the middle because the electric field is maximum there and becomes zero at the side walls. This value will be increased, however, when a dielectric material is placed on both sides of the ridge as is done in a TWM. The increase depends on the distance the material extends from the side walls to the ridge and also on the distance from the ladder line to the bottom plate.

From transmission line theory, the characteristic impedance Z_0 of Equation 11 can be approximately expressed as

$$Z_0 \approx 120 \ln \frac{x}{t} \tag{13}$$

where t = the thickness of the ladder line. Thus, CZ_0, which appears in Equation 11, can be written as

$$CZ_0 = \frac{120\epsilon cp}{d}\left(1 - \frac{x}{p}\right) \ln \frac{x}{t} \tag{14}$$

Thus for a certain set of dimensions of the structure, f_c, f_1, and CZ_0 can be calculated so that Equation 11 can be used to calculate a phase shift vs. frequency curve. From this plot the group velocity can be calculated at any frequency in the passband. Several of these curves have been plotted and are presented in Figures 6-9.

5
PHASE SHIFT vs. FREQUENCY for the KARP STRUCTURE

Figure 6 illustrates the effect of CZ_0 on the characteristics of the structure. It can be seen from these curves that for a certain lower cutoff frequency, f_c, and a certain f_1, the upper cutoff frequency is decreased when CZ_0 is increased. This decreases the structure passband and higher slowing factors result. CZ_0 is related to the structure dimensions and to the dielectric constant of the material through Equation 14.

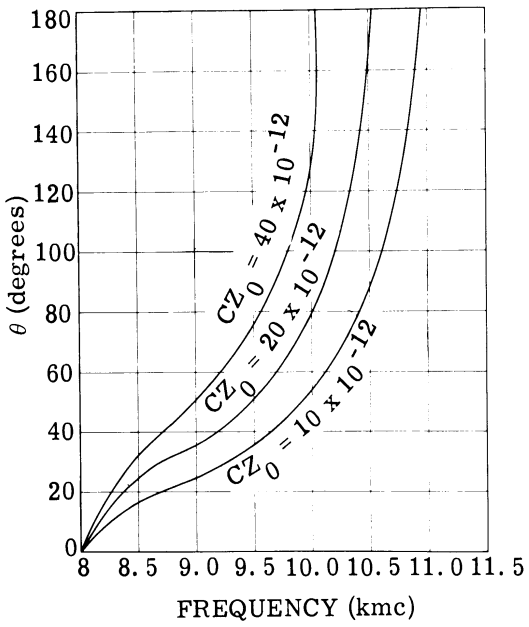

FIGURE 6. PHASE SHIFT PER SECTION θ, vs. FREQUENCY WITH CZ_0 AS A PARAMETER. f_c = 8 kmc, f_1 = 11 kmc.

It is obvious from this relation that CZ_0 can be increased in several ways. One way is to decrease d, the distance between the ladder and the ridge. This, however, has a slightly negative effect in that the lower cutoff frequency is decreased when d is decreased while the other dimensions are kept the same. The net effect is favorable, however, because the upper cutoff frequency decreases more rapidly than the lower one, which results in the passband becoming narrower. This effect is illustrated in Figure 7.

Another way to increase CZ_0 is to increase the dielectric constant of the material between the ridge and the ladder. This has the same effect as decreasing d.

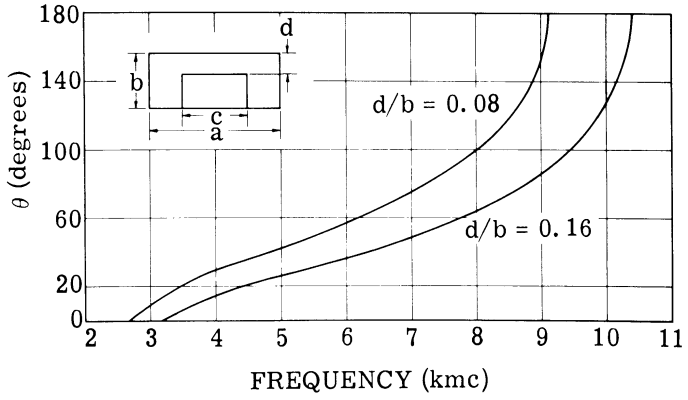

FIGURE 7. PHASE SHIFT PER SECTION, θ, vs. FREQUENCY WITH d AS A PARAMETER

The group velocity, v_g, which can be easily derived from Equation 11, is expressed as follows:

$$\frac{v_g}{p} = \frac{\left(2\pi f\left\{\frac{8}{CZ_0} - 2\pi f\left[1 - \left(\frac{f_c}{f}\right)^2\right]\tan\left(\frac{\pi}{2}\frac{f}{f_1}\right)\right\}\right)^{1/2}}{\left\{\left[1 - \left(\frac{f_c}{f}\right)^2\right]\left[\tan\left(\frac{\pi}{2}\frac{f}{f_1}\right)\right]\right\}^{1/2}\left[\frac{1 + \left(\frac{f_c}{f}\right)^2}{1 - \left(\frac{f_c}{f}\right)^2} + \frac{\frac{\pi f}{f_1}}{\sin\frac{\pi f}{f_1}}\right]} \qquad (15)$$

Graphs of v_g/p vs. frequency for different values of CZ_0 and specified values of f_c and f_1 are shown in Figure 8. These plots show that v_g can be made as small as desirable, either by decreasing p or by increasing CZ_0, while keeping f_c fixed. There are limits, however, on how small the pitch can be made. These were mentioned in Section 3. CZ_0 can be increased without affecting the lower cutoff frequency by increasing the ratio x/t.

It has been found that the passband can be narrowed and that higher slowing factors can be obtained by properly loading the structure with a dielectric material. This is illustrated in Figure 9, where the characteristic of an unloaded structure is compared with that of a ruby-loaded structure. For the unloaded structure the lower and upper cutoff frequencies were measured and found to be 8.5 and 12.5 kmc respectively. The loaded structure showed a lower cutoff frequency of 7 kmc and an upper cutoff frequency of 10 kmc. This structure was employed in the TWM experiments. Detailed discussions of the TWM assembly, the double-ridge Karp structure, and the experimental results are given in the following sections.

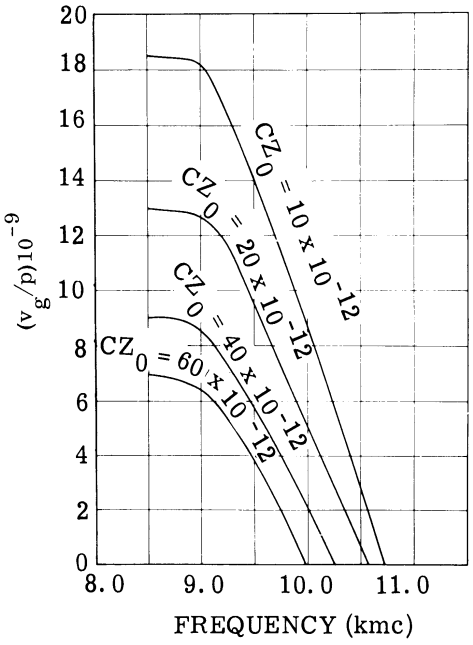

FIGURE 8. v_g/p VS. FREQUENCY FOR VARIOUS VALUES OF CZ_0. p is the pitch. f_c = 8 kmc, f_1 = 11 kmc.

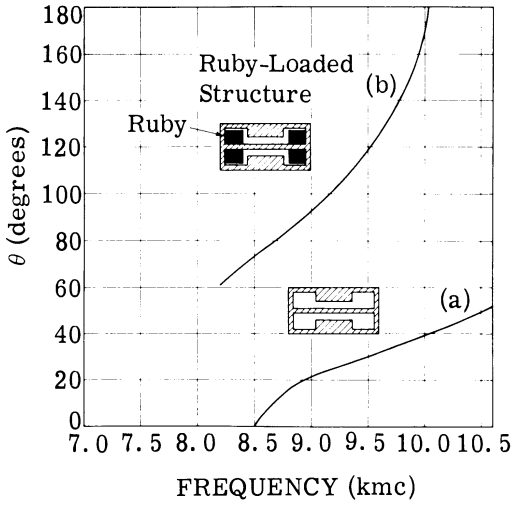

FIGURE 9. PHASE SHIFT PER SECTION, θ, vs. FREQUENCY FOR THE DOUBLE-RIDGE KARP STRUCTURE

6
TRAVELING-WAVE MASER ASSEMBLY

A double-ridge Karp-type slow-wave structure was employed in the TWM experiments. The ladder line of this structure has an over-all length of 4 inches, but the effective length of the interaction region is approximately 3.5 inches because the diameter of the pole pieces of the magnet is only 4 inches. The ladder line is photo-etched and made out of copper. It has a pitch of 0.040 inch, a separation between fingers of 0.020 inch, and a finger length of 0.44 inch. The phase shift vs. frequency characteristics of this structure are given in Figure 9.

The active material is light ruby, which has approximately 0.05% Cr^{+++} concentration. Both dark ruby, which has approximately 1% Cr^{+++} concentration, and polycrystalline yttrium iron garnet have been used for isolation.

An assembly view of the TWM is shown in Figure 10. The two coaxial lines provide the input and output coupling of the signal power to the structure. A sliding short which is adjustable by a screw movement, as well as the K-band waveguide through which the pump power is coupled into the structure, can also be seen in this figure. A provision for lowering the liquid

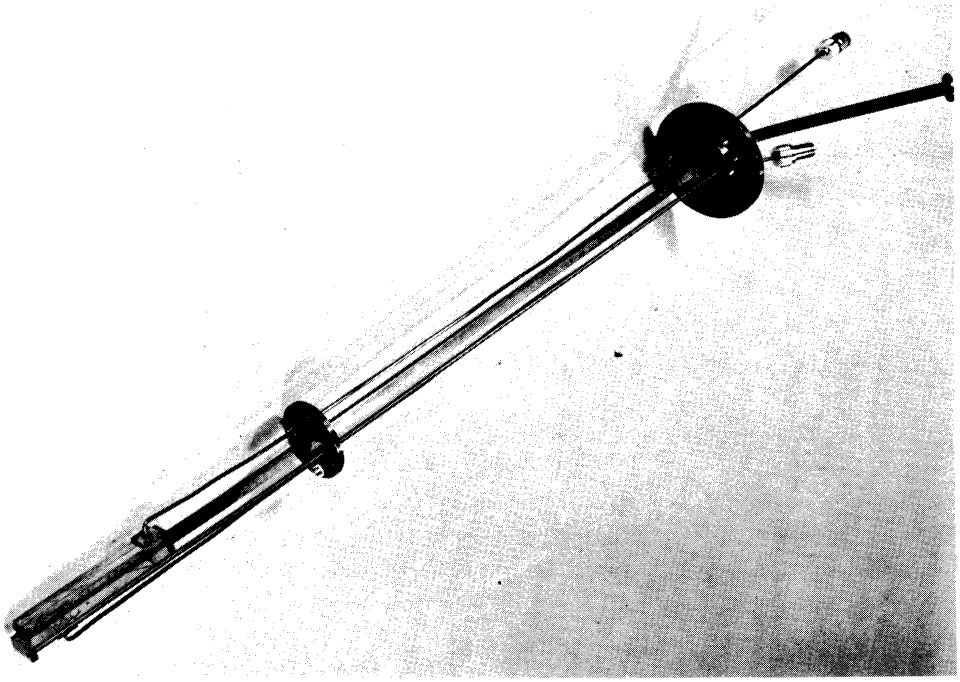

FIGURE 10. ASSEMBLED TRAVELING-WAVE MASER

helium temperature by using a large forepump in a closed cryogenic system has also been included in the assembly. However, no provision has been made to measure the absolute value of the bath temperature.

A closeup of the interaction region is presented in the disassembled views of Figure 11, and the coupling of the signal power into and out of the structure is clearly shown. The outer conductors of the coaxial lines are terminated at one side wall of the structure, while the center conductors extend to the other side wall. These portions of the center conductors are flattened out to the desired thickness and located in the plane of the ladder. Figure 11(b) shows the location of the flattened portions relative to the ladder line.

The location of the ruby crystals is also shown in the above figures. Two slabs (each 2 inches long) of light ruby, which is the active material, are placed on each side of the ridge of the bottom plate. These slabs extend all the way along the 4-inch ladder line and are located so that they touch the fingers. The four slabs of dark ruby which provide the isolation are similarly located in the top plate and do not touch the fingers but are very close to them. In recent experiments, however, the dark ruby slabs have been replaced by light ruby, and a slab of polycrystalline yttrium iron garnet was placed beside the ruby pieces in the top plate to provide the necessary isolation.

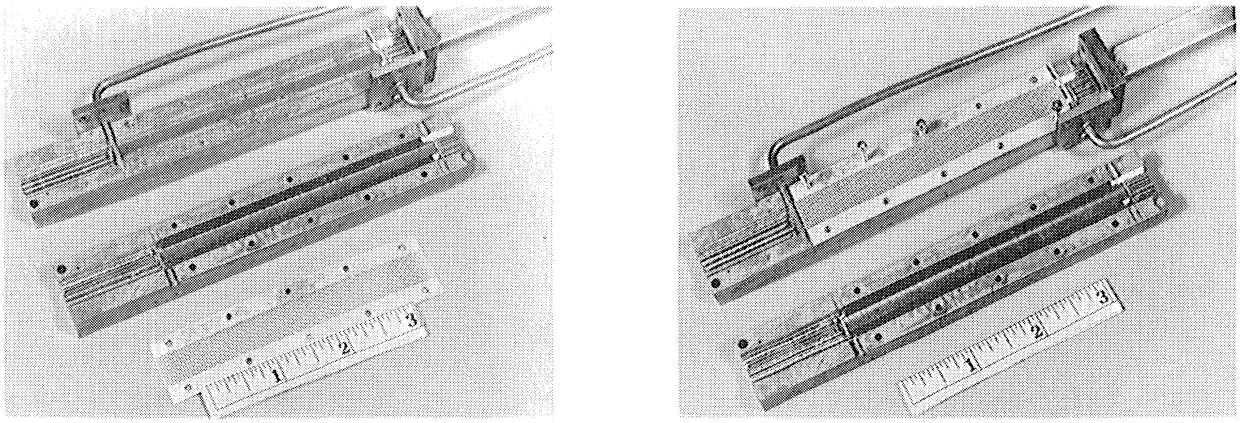

FIGURE 11. DISASSEMBLED TRAVELING-WAVE MASER. (a) The ladder line and the location of the ruby crystals. (b) The ladder line in position and the top plate at the side.

Figure 11(b) shows the ladder line in place and the top plate. This top plate fits over the ladder and is attached to the bottom plate with screws. The K-band waveguide is connected to the structure on one end and the pump power propagates through the structure in a ridged-waveguide mode. The other end of the structure is terminated by an adjustable sliding short.

7
EXPERIMENTAL RESULTS

With the coupling scheme described in Section 6, standing-wave ratios of 1.5-2.0 were obtained over quite a wide frequency range. The VSWR (voltage standing-wave ratio) was found to vary quite abruptly over the passband of the structure, but adequate matching was obtained at the desired signal frequencies by adjusting both the thickness of the flattened portion of the center conductor and its relative position with respect to the ladder line. The appearance of the passband was improved when an isolating material was incorporated into the structure. The isolating material suppresses the internal resonances in the structure. This is illustrated in Figure 12, where Figure 12(a) is the transmitted power for zero magnetic field, Figure 12(b) is for the magnetic field in the reverse direction, and Figure 12(c) is for the magnetic field in the normal direction. The isolating material in this case was dark ruby and pump power was applied.

The point on the energy level diagram employed in these experiments was the push-pull point (References 9 and 10). This point occurs when the angle between the d-c magnetic field and the ruby c-axis is approximately 55°. At this point of operation and for a pump frequency

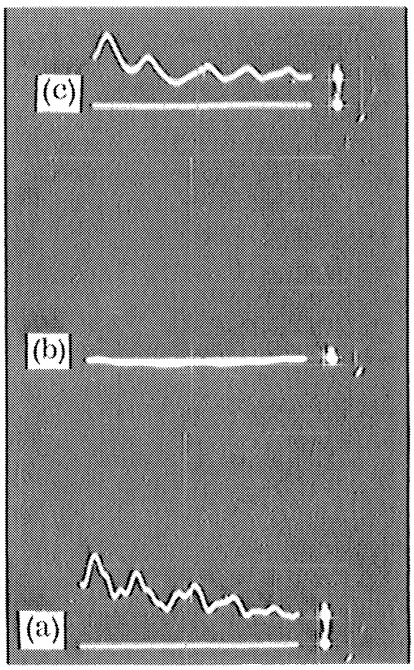

FIGURE 12. THE OUTPUT POWER FROM THE SLOW-WAVE STRUCTURE SHOWING THE EFFECT OF THE DARK RUBY ISOLATOR

of approximately 24 kmc, the corresponding signal frequency is around 9.65 kmc and the magnetic field is near 4.1 kilogauss.

The insertion loss in the neighborhood of the signal frequency is approximately 11-13 db at room temperature. At liquid helium temperatures this loss decreased to 8-9 db. This loss includes the input and output coaxial lines, which have an attenuation of approximately 0.4 db per foot at room temperature. A total of approximately 7 feet of coaxial line was used. The insertion loss can be made lower by using waveguides instead of coaxial cables to couple the signal power into and out of the structure, but this would make the maser assembly and dewar quite bulky. A better way to improve the loss in the structure would be to improve the assembly. Since the magnetic fields are strongest at the side walls where the top and bottom plates are fastened together, a very good contact at these points will minimize the losses. The screws alone might not provide a good contact.

When four slabs of dark ruby (two slabs placed on each side of the ridge of the top plate as shown in Figure 11(b) were employed for isolation, an absorption of 16-17 db was obtained with the d-c magnetic field in the reverse direction, and an absorption of approximately 2 db was obtained with the field in the normal direction. These values of absorption were obtained

at a bath temperature of 4.2°K, and the results are shown in Figure 12. Even though the dark ruby material provides good isolation it was found difficult to align the c-axes of the several ruby crystals in order to obtain amplification from the light ruby and absorption from the dark ruby at the same value of magnetic field. The dark ruby also absorbs an appreciable amount of pump power, which renders its application as the isolating material less attractive.

In recent experiments on the TWM, the dark ruby pieces in the top plate were replaced by light ruby pieces. A slab of yttrium iron garnet, cut to the proper size for ferromagnetic resonance and placed beside the light ruby pieces on one side of the ridge in the top plate, was employed for isolation. A forepump was employed to pump the liquid helium in order to reduce its temperature. It was observed that the electronic gain was 2.5 times higher with the forepump than without it. As mentioned previously the dewar design did not include a provision for measuring the absolute value of the temperature.

A high degree of nonreciprocity was achieved by using the garnet slab. When the structure was operated simply as an isolator the ratio of the absorption in the backward direction to that in the forward direction was approximately 15. The addition of the garnet slab greatly improved the passband of the structure.

When the maser was operated with no isolation, a high degree of regeneration and very large amounts of regenerative gain and oscillations were observed. The bandwidth, on the other hand, decreased sharply. When sufficient isolation was incorporated in the structure, gross gains of 15 db over a bandwidth of 75 mc were obtained. The square-root gain bandwidth was 420 mcs. This amount of gain was obtained, however, at two slightly different signal frequencies by changing the d-c magnetic field while holding the pump frequency fixed.

Also, for a certain signal frequency, gross gains of approximately 15 db over a 75-mc bandwidth were obtained at two slightly different values of d-c magnetic field and at two corresponding values of pump frequency. This is attributed to the misalignment of the c-axes of the light ruby slabs. Figures 13 and 14 clearly illustrate the results mentioned above.

It can be deduced from the above results that if the c-axes of the ruby slabs were well aligned, gross gains of approximately 30 db over a bandwidth of possibly 35-40 mc could have been obtained. This corresponds to a $G^{1/2}B$ of greater than 1100. Attempts to align the c-axes of the available ruby slabs have failed so far, but alignment is certainly possible.

In one of the experiments, the c-axes of the ruby slabs were close enough together to result in gross gains of approximately 13 db over 130 mc bandwidth ($G^{1/2}B = 585$). By slightly

changing the magnetic field the gain was increased to 16 db over 70 mc. The total loss in the structure, including the isolator, was approximately 8 db, which left a net gain of 5 db over 130 mc in one case and a net gain of 8 db over 70 mc in the other. This is illustrated in Figure 15.

The amplification in the TWM can be tuned over a frequency range of 9.45 to 9.85 kmc (400 mc) by adjusting the pump frequency and the magnetic field.

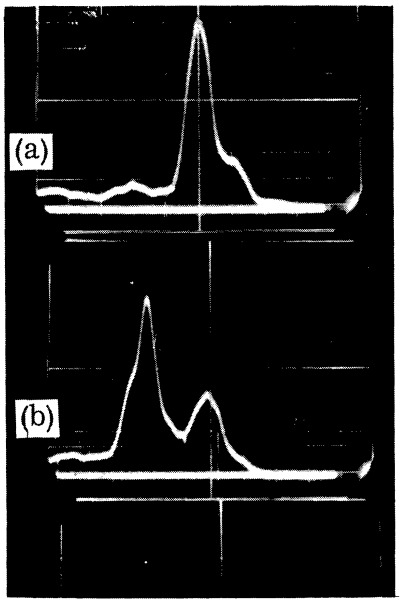

FIGURE 13. ELECTRONIC GAIN IN THE TWM, CASE 1. (a) The gain at a certain signal frequency and at corresponding values of d-c magnetic field and pump frequency. (b) The gain at a slightly higher signal frequency and at a slightly different value of d-c magnetic field but at the same pump frequency.

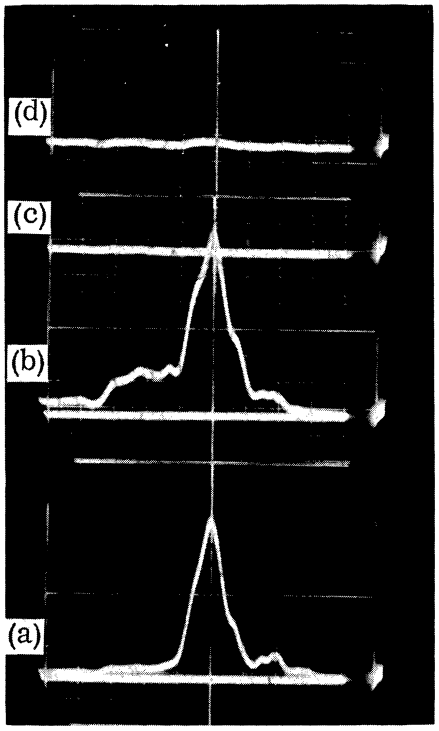

FIGURE 14. ELECTRONIC GAIN IN THE TWM, CASE 1. (a) The gain at a certain signal frequency and at corresponding values of d-c magnetic field and pump frequency. (b) The gain at the same signal frequency but at slightly different values of d-c magnetic field and pump frequency. (c) The output of the TWM with zero pump power but with the d-c magnetic field adjusted to resonance. (d) The output with zero field applied.

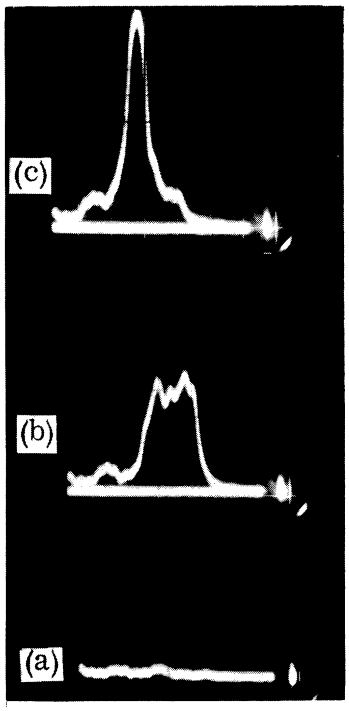

FIGURE 15. ELECTRONIC GAIN IN THE TWM, CASE 3. (a) The output power with zero d-c magnetic field. (b) The output with d-c field adjusted to resonance and pump power on. (c) The output at a slightly different value of magnetic field.

8
CONCLUSIONS

It can be concluded that operation of a TWM at X-band utilizing a Karp-type slow-wave structure is feasible. Gross gains of 30 db over a 35-mc ($G^{1/2}B \approx 1100$) bandwidth can be obtained at the push-pull point of operation. Even broader bandwidths can be achieved by stagger-tuning either the magnetic field or the ruby crystals. The major difficulty has been the alignment of the c-axes of the several ruby slabs, a difficulty which can certainly be minimized by a more careful procedure in cutting the pieces. The use of either dark ruby or polycrystalline yttrium iron garnet as the isolating material has been demonstrated and both were found feasible.

Gross rather than net gain has been emphasized in the measurements because this gives a better measure of the effectiveness of the slow-wave structure as a wave-slowing device. The circuit losses can be improved by fabrication and assembly techniques.

The application of a Karp-type slow-wave structure as a TWM circuit can be easily extended into the millimeter wave range. In this range, a very small length of the structure would be required to obtain adequate gain.

REFERENCES

1. N. Bloembergen, "Proposal for a New-Type Solid State Maser," Phys. Rev., October 1956, Vol. 104, p. 324.
2. H. E. D. Scovil, G. Feher, and H. Seidel, "Operation of a Solid State Maser," Phys. Rev., January 1957, Vol. 105, p. 762.
3. H. E. D. Scovil, "The Three-Level Solid State Maser," IRE Trans. on Microwave Theory and Tech., January 1958, Vol. MTT-6, No. 1, p. 29.
4. W. S. C. Chang, J. Cromack, and A. E. Siegman, "Cavity and Traveling-Wave Masers Using Ruby at S-Band," 1959 IRE WESCON Convention Record, Part 1, p. 142.
5. R. W. Degrasse, E. O. Schulz-Dubois, and H. E. D. Scovil, "The Three-Level Solid State Traveling-Wave Maser," Bell Telephone System, Tech. Publs. Monographs, March 1959, Vol. 38, No. 3213.

6. H. D. Tenney, R. Roberts, and P. H. Vartanian, "An S-Band Traveling-Wave Maser," 1959 IRE WESCON Convention Record, Part 1, p. 151.

7. N. Marcuvitz, Waveguide Handbook, MIT Radiation Laboratory Series, McGraw-Hill, New York, N. Y., 1951, Vol. 10, p. 400.

8. S. Hopfer, "The Design of Ridged Waveguides," IRE Trans. on Microwave Theory and Tech., October 1955, Vol. MTT-3, No. 5, pp. 20-29.

9. W. S. Chang and A. E. Siegman, Characteristics of Ruby for Maser Applications, Technical Report Number 156-2, Electron Devices Laboratory, Stanford University, Stanford, Calif., September 1958 (UNCLASSIFIED).

10. C. Kikuchi, J. Lambe, G. Makhov, and R. W. Terhune, "Ruby as a Maser Material," J. Appl. Phys., July 1959, Vol. 30, p. 1061.

PROJECT MICHIGAN DISTRIBUTION LIST 5
1 February 1961 — Effective Date

Copy No.	Addressee
1	Army Research Office, ORCD, DA Washington 25, D. C. ATTN: Research Support Division
2	Office, Assistant Chief of Staff for Intelligence Department of the Army, Washington 25, D. C. ATTN: Chief, Research & Development Branch
3	Commanding General, U. S. Continental Army Command Fort Monroe, Virginia ATTN: ATSWD-G
4-5	Commanding General U. S. Army Combat Surveillance Agency 1124 N. Highland Street Arlington 1, Virginia
6-8	Office of the Chief Signal Officer Department of the Army, Washington 25, D. C.
(6)	ATTN: Chief, Combat Development Branch, Research & Development Division
(7-8)	ATTN: Chief, Signal Research Office Research & Development Division
9-37	Commanding Officer U. S. Army Signal Research & Development Laboratory Fort Monmouth, New Jersey ATTN: SIGRA/SL-ADT
38-39	Commanding General U. S. Army Electronic Proving Ground Fort Huachuca, Arizona ATTN: Technical Library
40	Director, Weapons Systems Evaluation Group Room 1E880, The Pentagon Washington 25, D. C.
41	Chief of Engineers Department of the Army, Washington 25, D. C. ATTN: Research & Development Division
42	Chief, Chief of Ordnance, Research & Development Division Department of the Army, Washington 25, D. C. ATTN: ORDTB, Research & Special Projects
43	Commanding Officer, Army Map Service, Corps of Engineers U. S. Army, Washington 25, D. C. ATTN: Document Library
44	Commanding General Quartermaster Research & Engineering Command U. S. Army, Natick, Massachusetts
45-46	Chief, U. S. Army Security Agency Arlington Hall Station, Arlington 12, Virginia
47-48	Commander, Army Rocket & Guided Missile Agency Redstone Arsenal, Alabama ATTN: Technical Library, ORDXR-OTL
49	Commanding Officer U. S. Army Transportation Research Command Fort Eustis, Virginia ATTN: Research Reference Center
50	Commanding General Ordnance Tank-Automotive Command, Detroit Arsenal 28251 Van Dyke Avenue Centerline, Michigan ATTN: Chief, ORDMC-RRS
51	Commanding Officer, Ordnance Weapons Command Rock Island, Illinois ATTN: ORDOW-GN
52	Commanding Officer U. S. Army Diamond Ordnance Fuze Laboratories Washington 25, D. C. ATTN: ORDTL-300
53-55	Director, U. S. Army Engineer Research & Development Laboratories Fort Belvoir, Virginia
(53)	ATTN: Chief, Topographic, Engineer Department
(54)	ATTN: Chief, Electrical Engineering Department
(55)	ATTN: Technical Documents Center
56	Director, Human Engineering Laboratory Aberdeen Proving Ground, Aberdeen, Maryland
57	Commandant, U. S. Army Command & General Staff College Fort Leavenworth, Kansas ATTN: Archives
58	Commandant, U. S. Army Infantry School Fort Benning, Georgia ATTN: Combat Developments Office
59-60	Assistant Commandant U. S. Army Artillery & Missile School Fort Sill, Oklahoma
61	Assistant Commandant, U. S. Army Air Defense School Fort Bliss, Texas
62	Commandant, U. S. Army Engineer School Fort Belvoir, Virginia ATTN: ESSY-L
63	President, U. S. Army Infantry Board Fort Benning, Georgia
64	President, U. S. Army Artillery Board Fort Sill, Oklahoma
65	President, U. S. Army Air Defense Board Fort Bliss, Texas

Distribution List 5, 1 February 1961 — Effective Date

Copy No.	Addressee
66	President, U. S. Army Aviation Board Fort Rucker, Alabama
67-68	President, U. S. Army Intelligence Board Fort Holabird, Baltimore 19, Maryland
69	Office, Deputy Chief of Naval Operations Department of the Navy The Pentagon, Washington 25, D. C. ATTN: Op-07T
70-73	Office of Naval Research, Department of the Navy 17th & Constitution Avenue, N. W. Washington 25, D. C.
(70-71)	ATTN: Code 463
(72-73)	ATTN: Code 461
74-76	Chief, Bureau of Ships Department of Navy, Washington 25, D. C.
(74)	ATTN: Code 335
(75)	ATTN: Code 684C
(76)	ATTN: Code 690
77	Director, U. S. Naval Research Laboratory Washington 25, D. C. ATTN: Code 2027
78	Commanding Officer U. S. Navy Ordnance Laboratory Corona, California ATTN: Library
79	Commanding Officer & Director U. S. Navy Electronics Laboratory San Diego 52, California ATTN: Library
80-81	Department of the Air Force, Headquarters, USAF Washington 25, D. C.
(80)	ATTN: AFDRT-ER
(81)	ATTN: AFOIN-1B1
82	Aerospace Technical Intelligence Center, U. S. Air Force Wright-Patterson AFB, Ohio ATTN: AFCIN-4B1a, Library
83-92	ASTIA (TIPCR) Arlington Hall Station, Arlington 12, Virginia
93-100	Commander, Wright Air Development Division Wright-Patterson AFB, Ohio
(93-96)	ATTN: WWDE
(97)	ATTN: WWAD-DIST
(98-100)	ATTN: WWRNOO (Staff Physicist)
101	Commander, Rome Air Development Center Griffiss AFB, New York ATTN: RCOIL-2
102	APGC (PGTRI) Eglin Air Force Base, Florida
103-106	Central Intelligence Agency 2430 E Street, N. W. Washington 25, D. C. ATTN: OCR Mail Room
107-112	National Aeronautics & Space Administration 1520 H Street, N. W. Washington 25, D. C.
113	Combat Surveillance Project Cornell Aeronautical Laboratory, Incorporated Box 168, Arlington 10, Virginia ATTN: Technical Library
114	The RAND Corporation 1700 Main Street Santa Monica, California ATTN: Library
115-116	Cornell Aeronautical Laboratory, Incorporated 4455 Genesee Street Buffalo 21, New York ATTN: Librarian VIA: Bureau of Naval Weapons Representative 4455 Genesee Street Buffalo 21, New York
117-118	Director, Human Resources Research Office The George Washington University P. O. Box 3596, Washington 7, D. C. ATTN: Library
119	Chief Scientist, Department of the Army Office of the Chief Signal Officer Research & Development Division, SIGRD-2 Washington 25, D. C.
120	Columbia University, Electronics Research Laboratories 632 W. 125th Street New York 27, New York ATTN: Technical Library VIA: Commander, Rome Air Development Center Griffiss AFB, New York ATTN: RCKCS
121	Coordinated Science Laboratory, University of Illinois Urbana, Illinois ATTN: Librarian VIA: ONR Resident Representative 605 S. Goodwin Avenue Urbana, Illinois
122	Polytechnic Institute of Brooklyn 55 Johnson Street Brooklyn 1, New York ATTN: Microwave Research Institute Library VIA: Air Force Office of Scientific Research Washington 25, D. C.

Distribution List 5, 1 February 1961 — Effective Date

Copy No.	Addressee
123	Visibility Laboratory, Scripps Institution of Oceanography University of California San Diego 52, California VIA: ONR Resident Representative University of California Scripps Institution of Oceanography, Bldg. 349 La Jolla, California
124-125	Bureau of Naval Weapons Department of the Navy, Washington 25, D. C.
(124)	ATTN: RTPA-31
(125)	ATTN: RAAV-323
126	Headquarters, Tactical Air Command Langley AFB, Virginia ATTN: TPL-RQD (Requirements)
127	Headquarters, Tactical Air Command Langley AFB, Virginia ATTN: TOCE (Communications-Electronics)
128	Office of the Director Defense Research & Engineering Technical Library Department of Defense, Washington 25, D. C.
129	The Ohio State University Antenna Laboratory 2024 Neil Avenue Columbus 10, Ohio ATTN: Security Officer VIA: Commander Wright Air Development Division Wright-Patterson AFB, Ohio ATTN: WWKSC
130	Cooley Electronics Laboratory University of Michigan Research Institute Ann Arbor, Michigan ATTN: Director
131	U. S. Continental Army Command Liaison Officer, Project MICHIGAN The University of Michigan P. O. Box 618, Ann Arbor, Michigan
132	Commanding Officer, U. S. Army Liaison Group, Project MICHIGAN The University of Michigan P. O. Box 618, Ann Arbor, Michigan

AD Div. 25/6

Institute of Science and Technology, U. of Michigan, Ann Arbor
X-BAND LADDER-LINE TRAVELING-WAVE MASER by G. I. Haddad and J. E. Rowe. Rept. of Proj. MICHIGAN. Feb 61. 21 p. incl. illus., 10 refs.
(Rept. no. 2900-239-T)
(Contract DA-36-039 SC-78801) Unclassified report

The factors to be considered in the design of a broadband traveling-wave solid-state maser are outlined, with particular consideration given to the choice of an rf propagating structure. Desirable structure characteristics for a TWM (traveling-wave maser) are low loss, high slowing, ease of coupling between the pump signal and the paramagnetic crystal, simple, rugged construction, and easily accessible regions of different senses of circular polarization of the rf magnetic field.

An X-band ruby TWM has been constructed and tested in which the rf structure is a double-ridge ladder line and the signal is coupled into and out of the structure with coaxial lines. The
(over)

UNCLASSIFIED

I. Title: Project MICHIGAN
II. Haddad, G. I., Rowe, J. E.
III. U. S. Army Signal Corps
IV. Contract DA-36-039 SC-78801

Armed Services Technical Information Agency
UNCLASSIFIED

AD Div. 25/6

Institute of Science and Technology, U. of Michigan, Ann Arbor
X-BAND LADDER-LINE TRAVELING-WAVE MASER by G. I. Haddad and J. E. Rowe. Rept. of Proj. MICHIGAN. Feb 61. 21 p. incl. illus., 10 refs.
(Rept. no. 2900-239-T)
(Contract DA-36-039 SC-78801) Unclassified report

The factors to be considered in the design of a broadband traveling-wave solid-state maser are outlined, with particular consideration given to the choice of an rf propagating structure. Desirable structure characteristics for a TWM (traveling-wave maser) are low loss, high slowing, ease of coupling between the pump signal and the paramagnetic crystal, simple, rugged construction, and easily accessible regions of different senses of circular polarization of the rf magnetic field.

An X-band ruby TWM has been constructed and tested in which the rf structure is a double-ridge ladder line and the signal is coupled into and out of the structure with coaxial lines. The
(over)

UNCLASSIFIED

I. Title: Project MICHIGAN
II. Haddad, G. I., Rowe, J. E.
III. U. S. Army Signal Corps
IV. Contract DA-36-039 SC-78801

Armed Services Technical Information Agency
UNCLASSIFIED

AD Div. 25/6

Institute of Science and Technology, U. of Michigan, Ann Arbor
X-BAND LADDER-LINE TRAVELING-WAVE MASER by G. I. Haddad and J. E. Rowe. Rept. of Proj. MICHIGAN. Feb 61. 21 p. incl. illus., 10 refs.
(Rept. no. 2900-239-T)
(Contract DA-36-039 SC-78801) Unclassified report

The factors to be considered in the design of a broadband traveling-wave solid-state maser are outlined, with particular consideration given to the choice of an rf propagating structure. Desirable structure characteristics for a TWM (traveling-wave maser) are low loss, high slowing, ease of coupling between the pump signal and the paramagnetic crystal, simple, rugged construction, and easily accessible regions of different senses of circular polarization of the rf magnetic field.

An X-band ruby TWM has been constructed and tested in which the rf structure is a double-ridge ladder line and the signal is coupled into and out of the structure with coaxial lines. The
(over)

UNCLASSIFIED

I. Title: Project MICHIGAN
II. Haddad, G. I., Rowe, J. E.
III. U. S. Army Signal Corps
IV. Contract DA-36-039 SC-78801

Armed Services Technical Information Agency
UNCLASSIFIED

AD Div. 25/6

Institute of Science and Technology, U. of Michigan, Ann Arbor
X-BAND LADDER-LINE TRAVELING-WAVE MASER by G. I. Haddad and J. E. Rowe. Rept. of Proj. MICHIGAN. Feb 61. 21 p. incl. illus., 10 refs.
(Rept. no. 2900-239-T)
(Contract DA-36-039 SC-78801) Unclassified report

The factors to be considered in the design of a broadband traveling-wave solid-state maser are outlined, with particular consideration given to the choice of an rf propagating structure. Desirable structure characteristics for a TWM (traveling-wave maser) are low loss, high slowing, ease of coupling between the pump signal and the paramagnetic crystal, simple, rugged construction, and easily accessible regions of different senses of circular polarization of the rf magnetic field.

An X-band ruby TWM has been constructed and tested in which the rf structure is a double-ridge ladder line and the signal is coupled into and out of the structure with coaxial lines. The
(over)

UNCLASSIFIED

I. Title: Project MICHIGAN
II. Haddad, G. I., Rowe, J. E.
III. U. S. Army Signal Corps
IV. Contract DA-36-039 SC-78801

Armed Services Technical Information Agency
UNCLASSIFIED

AD

pump power is propagated in a waveguide mode, and the device is operated at and below liquid-helium temperatures. A 4-inch electromagnet was used. The TWM was operated at the push-pull point with a pump frequency of 24 kmc and a signal frequency of approximately 9.65 kmc; the magnetic field was 4.1 kilogauss.

Gross gains of 15 db have been obtained, and bandwidths as high as 130 mc were observed. Reduced structure losses and longer sections of ruby promise a $G^{1/2}B$ of 1100 mcs (30 db over 35 mc).

UNCLASSIFIED

DESCRIPTORS

Paramagnetic crystals
Radiofrequency amplifiers
Ruby
X-band

UNCLASSIFIED

AD

pump power is propagated in a waveguide mode, and the device is operated at and below liquid-helium temperatures. A 4-inch electromagnet was used. The TWM was operated at the push-pull point with a pump frequency of 24 kmc and a signal frequency of approximately 9.65 kmc; the magnetic field was 4.1 kilogauss.

Gross gains of 15 db have been obtained, and bandwidths as high as 130 mc were observed. Reduced structure losses and longer sections of ruby promise a $G^{1/2}B$ of 1100 mcs (30 db over 35 mc).

UNCLASSIFIED

DESCRIPTORS

Paramagnetic crystals
Radiofrequency amplifiers
Ruby
X-band

UNCLASSIFIED

AD

pump power is propagated in a waveguide mode, and the device is operated at and below liquid-helium temperatures. A 4-inch electromagnet was used. The TWM was operated at the push-pull point with a pump frequency of 24 kmc and a signal frequency of approximately 9.65 kmc; the magnetic field was 4.1 kilogauss.

Gross gains of 15 db have been obtained, and bandwidths as high as 130 mc were observed. Reduced structure losses and longer sections of ruby promise a $G^{1/2}B$ of 1100 mcs (30 db over 35 mc).

UNCLASSIFIED

DESCRIPTORS

Paramagnetic crystals
Radiofrequency amplifiers
Ruby
X-band

UNCLASSIFIED

AD

pump power is propagated in a waveguide mode, and the device is operated at and below liquid-helium temperatures. A 4-inch electromagnet was used. The TWM was operated at the push-pull point with a pump frequency of 24 kmc and a signal frequency of approximately 9.65 kmc; the magnetic field was 4.1 kilogauss.

Gross gains of 15 db have been obtained, and bandwidths as high as 130 mc were observed. Reduced structure losses and longer sections of ruby promise a $G^{1/2}B$ of 1100 mcs (30 db over 35 mc).

UNCLASSIFIED

DESCRIPTORS

Paramagnetic crystals
Radiofrequency amplifiers
Ruby
X-band

UNCLASSIFIED

AD Div. 25/6

Institute of Science and Technology, U. of Michigan, Ann Arbor
X-BAND LADDER-LINE TRAVELING-WAVE MASER by G. I. Haddad and J. E. Rowe. Rept. of Proj. MICHIGAN. Feb 61.
21 p. incl. illus., 10 refs.
(Rept. no. 2900-239-T)
(Contract DA-36-039 SC-78801) Unclassified report

The factors to be considered in the design of a broadband traveling-wave solid-state maser are outlined, with particular consideration given to the choice of an rf propagating structure. Desirable structure characteristics for a TWM (traveling-wave maser) are low loss, high slowing, ease of coupling between the pump signal and the paramagnetic crystal, simple, rugged construction, and easily accessible regions of different senses of circular polarization of the rf magnetic field.

An X-band ruby TWM has been constructed and tested in which the rf structure is a double-ridge ladder line and the signal is coupled into and out of the structure with coaxial lines. The (over)

UNCLASSIFIED

I. Title: Project MICHIGAN
II. Haddad, G. I., Rowe, J. E.
III. U. S. Army Signal Corps
IV. Contract DA-36-039 SC-78801

Armed Services Technical Information Agency
UNCLASSIFIED

AD Div. 25/6

Institute of Science and Technology, U. of Michigan, Ann Arbor
X-BAND LADDER-LINE TRAVELING-WAVE MASER by G. I. Haddad and J. E. Rowe. Rept. of Proj. MICHIGAN. Feb 61.
21 p. incl. illus., 10 refs.
(Rept. no. 2900-239-T)
(Contract DA-36-039 SC-78801) Unclassified report

The factors to be considered in the design of a broadband traveling-wave solid-state maser are outlined, with particular consideration given to the choice of an rf propagating structure. Desirable structure characteristics for a TWM (traveling-wave maser) are low loss, high slowing, ease of coupling between the pump signal and the paramagnetic crystal, simple, rugged construction, and easily accessible regions of different senses of circular polarization of the rf magnetic field.

An X-band ruby TWM has been constructed and tested in which the rf structure is a double-ridge ladder line and the signal is coupled into and out of the structure with coaxial lines. The (over)

UNCLASSIFIED

I. Title: Project MICHIGAN
II. Haddad, G. I., Rowe, J. E.
III. U. S. Army Signal Corps
IV. Contract DA-36-039 SC-78801

Armed Services Technical Information Agency
UNCLASSIFIED

AD Div. 25/6

Institute of Science and Technology, U. of Michigan, Ann Arbor
X-BAND LADDER-LINE TRAVELING-WAVE MASER by G. I. Haddad and J. E. Rowe. Rept. of Proj. MICHIGAN. Feb 61.
21 p. incl. illus., 10 refs.
(Rept. no. 2900-239-T)
(Contract DA-36-039 SC-78801) Unclassified report

The factors to be considered in the design of a broadband traveling-wave solid-state maser are outlined, with particular consideration given to the choice of an rf propagating structure. Desirable structure characteristics for a TWM (traveling-wave maser) are low loss, high slowing, ease of coupling between the pump signal and the paramagnetic crystal, simple, rugged construction, and easily accessible regions of different senses of circular polarization of the rf magnetic field.

An X-band ruby TWM has been constructed and tested in which the rf structure is a double-ridge ladder line and the signal is coupled into and out of the structure with coaxial lines. The (over)

UNCLASSIFIED

I. Title: Project MICHIGAN
II. Haddad, G. I., Rowe, J. E.
III. U. S. Army Signal Corps
IV. Contract DA-36-039 SC-78801

Armed Services Technical Information Agency
UNCLASSIFIED

AD Div. 25/6

Institute of Science and Technology, U. of Michigan, Ann Arbor
X-BAND LADDER-LINE TRAVELING-WAVE MASER by G. I. Haddad and J. E. Rowe. Rept. of Proj. MICHIGAN. Feb 61.
21 p. incl. illus., 10 refs.
(Rept. no. 2900-239-T)
(Contract DA-36-039 SC-78801) Unclassified report

The factors to be considered in the design of a broadband traveling-wave solid-state maser are outlined, with particular consideration given to the choice of an rf propagating structure. Desirable structure characteristics for a TWM (traveling-wave maser) are low loss, high slowing, ease of coupling between the pump signal and the paramagnetic crystal, simple, rugged construction, and easily accessible regions of different senses of circular polarization of the rf magnetic field.

An X-band ruby TWM has been constructed and tested in which the rf structure is a double-ridge ladder line and the signal is coupled into and out of the structure with coaxial lines. The (over)

UNCLASSIFIED

I. Title: Project MICHIGAN
II. Haddad, G. I., Rowe, J. E.
III. U. S. Army Signal Corps
IV. Contract DA-36-039 SC-78801

Armed Services Technical Information Agency
UNCLASSIFIED

AD

pump power is propagated in a waveguide mode, and the device is operated at and below liquid-helium temperatures. A 4-inch electromagnet was used. The TWM was operated at the push-pull point with a pump frequency of 24 kmc and a signal frequency of approximately 9.65 kmc; the magnetic field was 4.1 kilogauss.

Gross gains of 15 db have been obtained, and bandwidths as high as 130 mc were observed. Reduced structure losses and longer sections of ruby promise a $G^{1/2}B$ of 1100 mcs (30 db over 35 mc).

UNCLASSIFIED

DESCRIPTORS

Paramagnetic crystals
Radiofrequency amplifiers
Ruby
X-band

UNCLASSIFIED

AD

pump power is propagated in a waveguide mode, and the device is operated at and below liquid-helium temperatures. A 4-inch electromagnet was used. The TWM was operated at the push-pull point with a pump frequency of 24 kmc and a signal frequency of approximately 9.65 kmc; the magnetic field was 4.1 kilogauss.

Gross gains of 15 db have been obtained, and bandwidths as high as 130 mc were observed. Reduced structure losses and longer sections of ruby promise a $G^{1/2}B$ of 1100 mcs (30 db over 35 mc).

UNCLASSIFIED

DESCRIPTORS

Paramagnetic crystals
Radiofrequency amplifiers
Ruby
X-band

UNCLASSIFIED

AD

pump power is propagated in a waveguide mode, and the device is operated at and below liquid-helium temperatures. A 4-inch electromagnet was used. The TWM was operated at the push-pull point with a pump frequency of 24 kmc and a signal frequency of approximately 9.65 kmc; the magnetic field was 4.1 kilogauss.

Gross gains of 15 db have been obtained, and bandwidths as high as 130 mc were observed. Reduced structure losses and longer sections of ruby promise a $G^{1/2}B$ of 1100 mcs (30 db over 35 mc).

UNCLASSIFIED

DESCRIPTORS

Paramagnetic crystals
Radiofrequency amplifiers
Ruby
X-band

UNCLASSIFIED

AD

pump power is propagated in a waveguide mode, and the device is operated at and below liquid-helium temperatures. A 4-inch electromagnet was used. The TWM was operated at the push-pull point with a pump frequency of 24 kmc and a signal frequency of approximately 9.65 kmc; the magnetic field was 4.1 kilogauss.

Gross gains of 15 db have been obtained, and bandwidths as high as 130 mc were observed. Reduced structure losses and longer sections of ruby promise a $G^{1/2}B$ of 1100 mcs (30 db over 35 mc).

UNCLASSIFIED

DESCRIPTORS

Paramagnetic crystals
Radiofrequency amplifiers
Ruby
X-band

UNCLASSIFIED